

Conductance and dielectric properties of hydrogen and hydroxyl passivated SiCNWs

Wan-Duo Ma(马婉铎), Ya-Lin Li(李亚林), Pei Gong(龚裴), Ya-Hui Jia(贾亚辉), and Xiao-Yong Fang(房晓勇)
Citation: Chin. Phys. B, 2021, 30 (**10**): 107801. DOI: 10.1088/1674-1056/abf130
Journal homepage: http://cpb.iphy.ac.cn; http://iopscience.iop.org/cpb

What follows is a list of articles you may be interested in

Enhanced mobility of MoS_2 field-effect transistors by combining defect passivation with dielectric-screening effect

Zhao Li(李钊), Jing-Ping Xu(徐静平), Lu Liu(刘璐), and Xin-Yuan Zhao(赵心愿)
Chin. Phys. B, 2021, 30 (**1**): 018102. DOI: 10.1088/1674-1056/abb30f

Crystalline silicon surface passivation investigated by thermal atomic-layer-deposited aluminum oxide

Cai-Xia Hou(侯彩霞), Xin-He Zheng(郑新和), Rui Jia(贾锐), Ke Tao(陶科), San-Jie Liu(刘三姐), Shuai Jiang(姜帅), Peng-Fei Zhang(张鹏飞), Heng-Chao Sun(孙恒超), Yong-Tao Li(李永涛)
Chin. Phys. B, 2017, 26 (**9**): 098103. DOI: 10.1088/1674-1056/26/9/098103

Studies on the polycrystalline silicon/SiO_2 stack as front surface field for IBC solar cells by two-dimensional simulations

Shuai Jiang(姜帅), Rui Jia(贾锐), Ke Tao(陶科), Caixia Hou(侯彩霞), Hengchao Sun(孙恒超), Zhiyong Yu(于志泳), Yongtao Li(李勇滔)
Chin. Phys. B, 2017, 26 (**8**): 087802. DOI: 10.1088/1674-1056/26/8/087802

Improved interfacial and electrical properties of GaSb metal oxide semiconductor devices passivated with acidic $(NH_4)_2S$ solution

Zhao Lian-Feng, Tan Zhen, Wang Jing, Xu Jun
Chin. Phys. B, 2014, 23 (**7**): 078102. DOI: 10.1088/1674-1056/23/7/078102

Electrospun fluorescein/polymer composite nanofibers and their photoluminescent properties

Zhang Zhi-Hua, Long Yun-Ze, Yin Hong-Xin, Sun Bin,Zheng Jie, Zhang Hong-Di, Ji Xin-Ming, Gu Chang-Zhi
Chin. Phys. B, 2012, 21 (**9**): 097805. DOI: 10.1088/1674-1056/21/9/097805

Conductance and dielectric properties of hydrogen and hydroxyl passivated SiCNWs*

Wan-Duo Ma(马婉铎), Ya-Lin Li(李亚林), Pei Gong(龚裴),
Ya-Hui Jia(贾亚辉), and Xiao-Yong Fang(房晓勇)†

Key Laboratory for Microstructural Material Physics of Hebei Province, School of Science, Yanshan University, Qinhuangdao 066004, China

(Received 12 January 2021; revised manuscript received 22 February 2021; accepted manuscript online 24 March 2021)

Based on the transport theory and the polarization relaxation model, the effects of hydrogen and hydroxyl passivation on the conductivity and dielectric properties of silicon carbide nanowires (SiCNWs) with different sizes are numerically simulated. The results show that the variation trend of conductivity and band gap of passivated SiCNWs are opposite to the scenario of the size effect of bare SiCNWs. Among the influencing factors of conductivity, the carrier concentration plays a leading role. In the dielectric properties, the bare SiCNWs have a strong dielectric response in the blue light region, while passivated SiCNWs show a more obvious dielectric response in the far ultraviolet-light region. In particular, hydroxyl passivation produces a strong dielectric relaxation in the microwave band, indicating that hydroxyl passivated SiCNWs have a wide range of applications in electromagnetic absorption and shielding.

Keywords: silicon carbide nanowires, passivation, conductance properties, dielectric relaxation

PACS: 78.67.Uh, 81.65.Rv, 87.16.Uv, 77.22.Gm **DOI:** 10.1088/1674-1056/abf130

1. Introduction

SiC nanomaterials, with high breakdown field strength, high thermal conductivity, wide band gap, small thermal expansion coefficient, small dielectric constant, good chemical stability, strong radiation resistance, and other good mechanical properties,[1–4] are typical IV–IV semiconductors. And they are used in light-emitting diode,[5] laser,[6,7] visible-light blind EUV and ultraviolet detectors,[8,9] microwave and millimeter-wave power devices.[10] Conductivity and dielectric constant are important parameters of high-frequency electronic devices. More and more attention is paid to the transport, recombination and dielectric microscopic mechanism of non-carbon nanomaterials such as silicon carbide with the development of micro-nano electronic technology.[11,12] However, the broken bonds (dangling bonds) on the surface of nanomaterials lead to instability of the surface. The enhancement of the surface activity of nanomaterials also restricts their applications in micro-nano devices, *etc*., and passivation or surface modification is an effective way to improve the stability of performance. Therefore, the study of passivated SiC nanomaterials, especially the influence of different passivating factors (atom or group) on the conductivity and dielectric properties of SiCNWs, is of great significance.[13]

The surface passivation of SiC has been studied for a long time. For instance, Gendron and Porte investigated the effects of hydrogen atom passivation on donors and recipients of SiC as early as 1995, and the results showed that hydrogen atom passivation leads the mobility of the SiC to increase.[14] In 2009, Trejo *et al*. studied the effects of passivation on the band gap of porous cubic silicon carbide and found that hydrogen passivation significantly changes the surface structure of SiC.[15] In 2012, Cuevas *et al.* studied the influence of hydrogen atom passivation and hydroxyl group passivation on 3C-SiC, and the results showed that the structure of hydroxyl passivation is more stable, and the band gap of the structure after passivation and the electronegativity of the passivated atoms are negatively correlated with each other.[16] In 2018, Li *et al.* studied the influence of hydrogen atom passivation on SiCNWs and their results demonstrated that hydrogen atom passivation turns SiCNWs into a direct band-gap semiconductor, and hydrogen atom passivation makes the optical properties of SiCNWs more stable.[17] In the same year, Cuevas *et al.* performed hydrogen and oxygen atom passivation in the [110] direction of 3C-SiCNWs, and their results showed that the passivation increases the photoactivity, the band gap of the structure passivated by oxygen atom at C position is smaller than that of the structure passivated by hydrogen atom, while the band gap of the structure passivated by oxygen atom at Si position is larger than that of the structure passivated by hydrogen atom, and the oxygen passivation leads the chemical stability of SiCNWs to increase.[18] Javan studied the effects of passivation on the electrical and optical properties of 3C-SiC nanocrystals in 2015, and the results showed that the structure passivated at Si position is more stable, and the functional groups adsorbed on the surface of SiC nanocrystals

*Project supported by the National Natural Science Foundation of China (Grant No. 11574261) and the Natural Science Foundation of Hebei Province, China (Grant No. A2021203030).

†Corresponding author. E-mail: fang@ysu.edu.cn

© 2021 Chinese Physical Society and IOP Publishing Ltd

changes the optical properties of SiC nanocrystals, especially the structures passivated by amides and mercaptan.[19] Jia *et al.* studied the effects of hydrogen passivation and hydroxyl passivation on structure, electrical and optical properties of SiCNWs in 2020, and found that passivation can improve the stability of SiCNWs' structure and enhance the stability of the optical properties, and lead the light absorption to decrease, moreover, the response peaks of photoconductivity and other spectra move to the deep ultraviolet region.[20] The reviews in the above-mentioned literature indicate that most of the studies of passivation of SiC nanomaterials focus on the stability of lattice structure and macroscopic properties such as electrical and optical properties, but only a few studies concentrate on the microscopic mechanisms such as electronic states and their polarization and carrier transport. Moreover, at the electronic level, there are a few reports on the effects of different passivation factors on the transport and dielectric relaxation properties of SiC nanomaterials.

In this paper, we use hydrogen and hydroxyl group to passivate the surfaces of SiCNWs with three different sizes. The conductivity and dielectric properties of the SiCNWs before and after passivation are numerically simulated according to the transport theory and polarization relaxation model. The effects of hydrogen and hydroxyl passivation on the conductivity and dielectrical property of the SiCNWs are revealed by analyzing the characteristics of bare, hydrogen and hydroxyl passivated SiCNWs, which provides a theoretical basis for broadening the application scope of SiC nanomaterials.

2. First-principles calculations

2.1. Model

This study uses the CASTEP module in Materials Studio 6.0 software to optimize and calculate the target model. The hexagonal cross section of a 2H-SiC ($3 \times 3 \times 2$) cell in the [001] direction is taken as the basic structure and is denoted as SiCNWs1. The surfaces are passivated with the hydroxy group and hydrogen atoms, respectively, and denoted correspondingly as H-SiCNWs1and OH-SiCNWs1. Moreover, construct the unit cells of $4 \times 4 \times 2$, $5 \times 5 \times 2$ hexagonal cross-sections with different diameters, denoted as SiCNWs2 and SiCNWs3, respectively, then the passivation structure will be named H-SiCNWs2 and OH-SiCNWs2, H-SiCNWs3 and OH-SiCNWs3.

2.2. Electronic structure of passivated SiCNWs

Figures 1 and 2 show band and electron density of bare SiCNWs and passivated SiCNWs based on first principles.

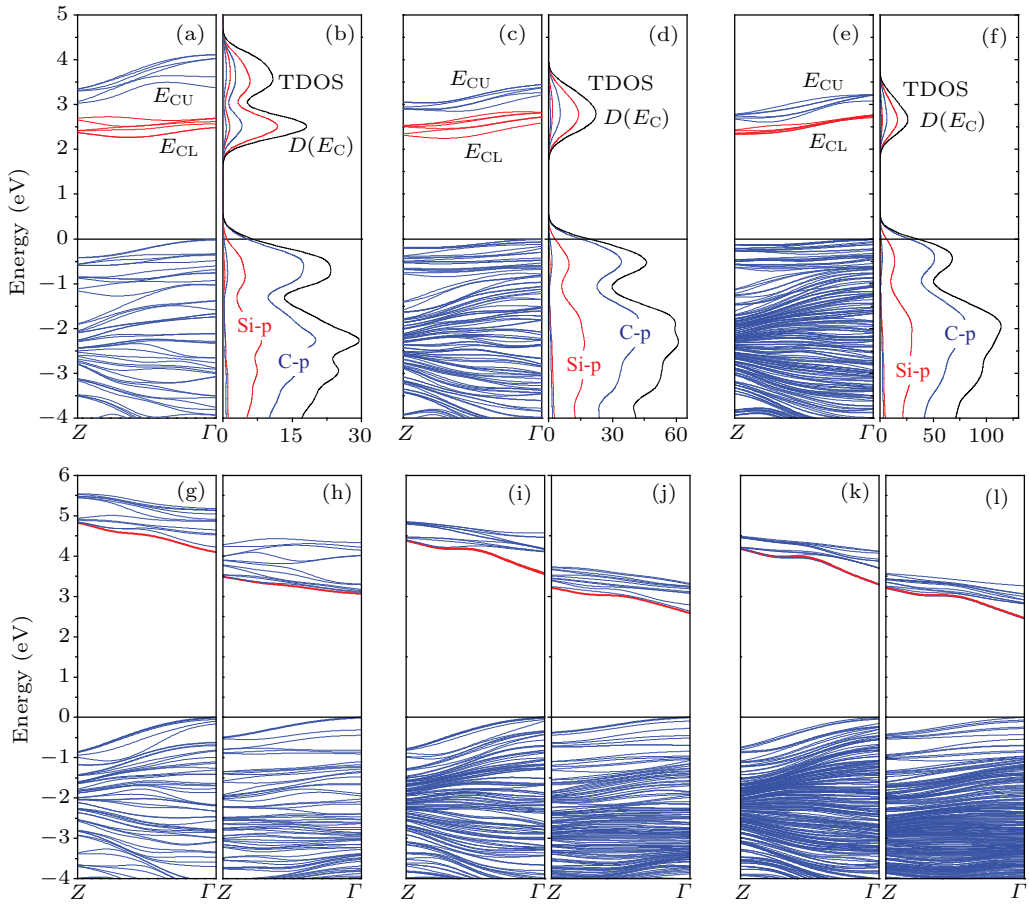


Fig. 1. Band structures and densities of electron states of unpassivated, hydrogen-passivated, and hydroxyl passivated SiCNWs with different diameters, showing band structures of (a) SiCNWs1, (c) SiCNWs2 and (e) SiCNWs3, and ((b), (d) and (f)) their corresponding densities of states, band structures of (g) H-SiCNWs1, (i) H-SiCNWs2, (k) H-SiCNWs3, (h) OH-SiCNWs1, (j) OH-SiCNWs2, and (l) OH-SiCNWs3.

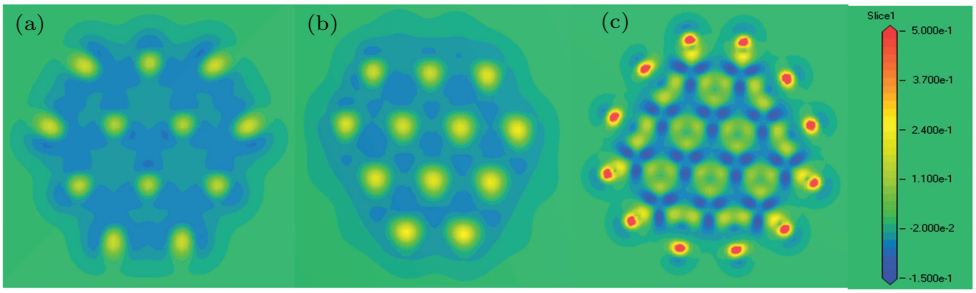


Fig. 2. Differential state density distribution of (a) unpassivated, (b) hydrogen-passivated, and (c) hydroxy-passivated SiCNWs.

Table 1. Electronic structure parameters of bare and passivated SiCNWs.

	V (nm^3)	c (nm)	E_g (eV)	m_e^* (m)	m_h^* (m)	$D(E_c)$ (eV^{-1})	p_{Si} (10^{-30} C·m)	p_C (10^{-30} C·m)
SiCNWs1	2.524	0.5113	2.258	0.72	3.85	18.05	–	–
SiCNWs2	2.702	0.5098	2.324	1.32	5.72	22.69	–	–
SiCNWs3	4.201	0.5090	2.342	1.59	6.44	26.68	–	–
H-SiCNWs1	2.468	0.5115	4.054	0.49	1.14	–		
H-SiCNWs2	2.747	0.5099	3.556	0.79	3.40	–		
H-SiCNWs3	4.349	0.5090	3.292	0.64	3.32	–		
OH-SiCNWs1	2.621	0.5205	3.062	1.36	1.49	—	13.43	6.12
OH-SiCNWs2	3.973	0.5162	2.587	0.84	2.71	–	12.99	5.80
OH-SiCNWs3	4.527	0.5136	2.459	0.72	3.82	–	13.07	5.87

According to Fig. 1, it can be seen that the bare SiCNWs are an indirect band gap semiconductor, in which the valence band top is in the center of Brillouin (Γ point) and the conduction band bottom is near the Brillouin boundary (Z point). Because of the dangling bonds on the bare SiCNWs' surfaces, conduction band bottom of bare SiCNWs is composed of discrete impurity bands.[21] Moreover, the dispersion of impurity bands decreases with the increase of diameter, which leads to a slight increase in the bottom of the conduction band as shown in Figs. 1(a), 1(c), and 1(e). The passivated SiCNWs are a direct band gap semiconductor. When the dangling bonds are saturated with hydrogen or hydroxyl, the impurity band disappears, resulting in the increase of SiCNWs' band-gap. Among them, the increase of the band gap of SiCNWs, caused by hydrogen passivation, is greater than that of hydroxyl passivation. Contrary to the size effect of bare SiCNWs, the band gap of the passivated SiCNWs decreases with diameter increasing as shown in Figs. 1(g)–1(l).

According to the electron density difference, it can be seen that the hydroxyl passivation lead the distinct intrinsic electric dipoles to be introduced into the surfaces of SiCNWs as shown in Fig. 2(c). This is because the electronegativity of hydrogen atom is close to that of Si and C atoms, which makes the hydrogen passivation to form a non-polar covalent bond. The first principles study shows that the C-OH bonds and the Si–OH bonds have relatively small population values, which indicates that they are polar covalent bonds. Therefore, hydroxyl passivation produces intrinsic electric dipoles, while hydrogen passivation does not produce dipoles. The electronic structure parameters based on the first principles study are shown in Table 1.

In the table, V is the supercell volume of SiCNWs, c is the lattice constant in the direction of [001], E_g is the band gap, m_e^* and m_h^* are the electron and hole effective masses, respectively, p_{Si} and p_C are the dipole moments formed by passivating the surface Si and C atoms, respectively. On the basis of the first principles data, the dipole moment produced by hydroxyl passivation at the C-position is different from that at the Si-position, and the dipole moment produced by the hydroxyl passivation at the C-position is smaller than that at the Si-passivation.

3. Conductive properties of different passivated SiCNWs

3.1. Conductivity of bare and passivated SiCNWs

The conductivity of semiconductor is determined by the carrier concentration and mobility, which can be expressed as

$$\sigma = en_e\mu_e + en_h\mu_h, \tag{1}$$

where n_e and μ_e are the electron concentration and its mobility, n_h and μ_h are the hole concentration and its mobility, respectively. For an intrinsic semiconductor, the electron concentration is the same as the hole concentration. From Ref. [22], the carrier concentration of SiC can be expressed as

$$n_e = n_h = \frac{\sqrt{2\pi k_B T}}{Sh}(m_e^* m_h^*)^{1/4}\exp\left(-\frac{E_g}{2k_B T}\right). \tag{2}$$

In Eq. (2), S is the cross-sectional area of the nanowire, k_B is the Boltzmann constant, h is the Planck constant.

The carrier mobility of SiCNWs is determined by the scattering mechanism, and it can be expressed as

$$\mu_{\mathrm{e}} = \frac{e}{m_{\mathrm{e}}^*}\tau_{\mathrm{e}} \quad \text{and} \quad \mu_{\mathrm{h}} = \frac{e}{m_{\mathrm{h}}^*}\tau_{\mathrm{h}}, \tag{3}$$

where τ_{e} and τ_{h} denote the relaxation time of electron scattering and the relaxation time of hole scattering, respectively. For bare SiCNWs, dangling bond on surface leads the impurity band to be discretized, so electron mobility can be expressed as[23]

$$\mu_{\mathrm{e}} = \frac{ev_{\mathrm{ph}}l^2}{6k_{\mathrm{B}}T}\exp\left(-2\alpha l - \frac{W}{k_{\mathrm{B}}T}\right), \tag{4}$$

where v_{ph} denotes the atomic vibration frequency (phonon frequency) and l refers to the electron transition distance (impurity spacing). The hopping activation energy W is determined by the electron density of states $D(\varepsilon_{\mathrm{c}})$ of the impurity band, that is, $W = 1/D(\varepsilon_{\mathrm{c}})$. The spatial extensibility of wave function $1/\alpha$ can be estimated from the uncertainty relation Δx. $\Delta p \geq h/2\pi$, that is $\alpha \leq 2\pi\delta/c$, where c is the lattice constant of SiCNWs, δ is the k-point accuracy determined by grid parameters.[23] For holes in valence bands, optical phonon scattering is the dominant transport mechanism, and the hole mobility can be obtained from Refs. [12,23], and expressed as

$$\mu_{\mathrm{h}} = \frac{\varepsilon_0 h^2\left(\mathrm{e}^{h\nu_{\mathrm{opt}}/k_{\mathrm{B}}T}-1\right)}{\pi e\left(2m^{*3}h\nu_{\mathrm{opt}}\right)^{1/2}}\frac{\varepsilon_{\mathrm{s}}\varepsilon_{\mathrm{opt}}}{\left(\varepsilon_{\mathrm{s}}-\varepsilon_{\mathrm{opt}}\right)}. \tag{5}$$

where ν_{opt} is the optical phonon frequency, e is the energy of the charge. ε_0, ε_{s}, and $\varepsilon_{\mathrm{opt}}$ are the vacuum dielectric constant, the static dielectric constant, and the optical-frequency related dielectric constant, respectively.

After the hydrogen passivation, the impurity band of the SiCNWs disappears. Hence, the electron concentration and hole concentration of the SiCNW are both determined from Eq. (2), and its mobility can be obtained from Eq. (5).

For the SiCNWs passivated by hydroxyl group, the carrier concentration is still determined from Eq. (2). Hydroxyl group is a polar group, in which there also exists (ionized) impurity scattering in SiCNWs, and the scattering probability can be expressed as

$$\frac{1}{\tau_{\mathrm{ion}}} = \frac{N_{\mathrm{ion}}e^4}{8\pi\left(m^*\varepsilon_0\varepsilon_{\mathrm{s}}\right)^2 v^3}\ln\left[1+\left(\frac{2\pi m^*\varepsilon_0\varepsilon_{\mathrm{s}}v^2}{N_{\mathrm{ion}}^{1/3}e^2}\right)^2\right], \tag{6}$$

where N_{ion} is ionized impurity density and v is the average carrier concentration of SiCNWs, which can be expressed as

$$\bar{v} = \left(\frac{9\pi k_{\mathrm{B}}T}{8m^*}\right)^{1/2}. \tag{7}$$

3.2. Temperature dependent conductivity

The transport properties of bare, hydrogen, and hydroxyl passivated SiCNWs are numerically simulated according to Eqs. (1)–(7) based on first-principles data. The results are shown in Figs. 3–5.

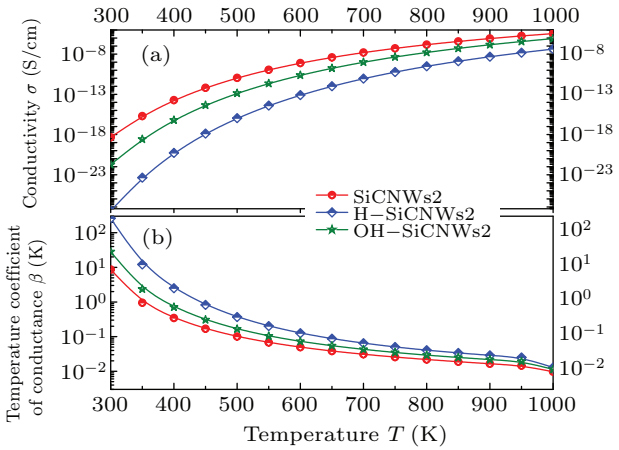


Fig. 3. (a) Temperature-dependent conductivity and (b) temperature-dependent coefficient of conductance of bare and passivated SiCNWs.

Figure 3 shows that in the temperature range of 300 K–1000 K, whether the SiCNWs are passivated or not, their conductivity has the temperature characteristics of a typical semiconductor, that is, the conductivity increases with temperature rising. Meanwhile, temperature coefficient of conductance (TCC) decreases rapidly, indicating that the larger the conductivity, the smaller the temperature drift is. At the same temperature, the conductivity of SiCNWs is larger than that of passivated SiCNWs, in which the conductivity of hydroxyl passivation SiCNWs is larger than that of hydrogen passivated SiCNWs. The two conductivity temperature coefficients are opposite to each other, the TCC value of the SiCNWs is the smallest, and the TCC value of the OH-SiCNWs and H-SiCNWs increase in turn.

Comparing Fig. 3(a) with Fig. 4(a), it can be seen that the main factor affecting the SiCNWs conductivity is the carrier concentration. Equation (2) shows that the smaller the band gap, the larger the intrinsic carrier concentration is, so the carrier concentration of bare SiCNWs is the largest among the carrier concentrations of three samples with the same size, while the carrier concentration of the hydrogen passivated SiCNWs is the smallest. Figure 4(b) shows that on the whole the electron mobility of the passivated SiCNWs is larger than the hole mobility, which is due to the fact that the effective mass of the electron is always smaller than that of the hole in the same semiconductor. However, the electron mobility of the bare SiCNWs is smaller than the hole mobility because they originate fom different transport mechanisms: the electrons are in the discrete impurity band and their mobilities are induced by the constant path hopping mechanism, while the holes are in the valence band of the continuous energy level and their mobilities are caused by the carrier scattering mechanism. In two different passivation methods, the optical phonon scattering plays a dominant role in the H-SiCNWs, in addition to the optical phonon scattering, there is ionizing impurity scattering in OH-SiCNWs, the scattering probability $1/\tau$

(the reciprocal of their scattering relaxation time) is shown in Fig. 4(c). Since the scattering probability of ionized impurity is much greater than that of optical phonon, the scattering of ionized impurity plays a dominant role in OH-SiCNWs. In the range of 300 K–1000 K, the scattering probability of ionized impurity decreases (the relaxation time increases correspondingly) with the increase of temperature, which leads the electron (hole) mobility to be enhanced. At the same time, the scattering probability of optical phonon increases (the relaxation time decreases correspondingly), and the mobility of H-SiCNWs decreases. Owing to the different carrier scattering mechanisms in the two passivated SiCNWs, the mobilities of the two passivated SiCNWs show opposite temperature dependence. In addition, owing to the high scattering probability of ionizing impurity and little difference in effective mass among electrons (holes) in passivated SiCNWs (see Table 1), OH-SiCNWs have a low mobility.

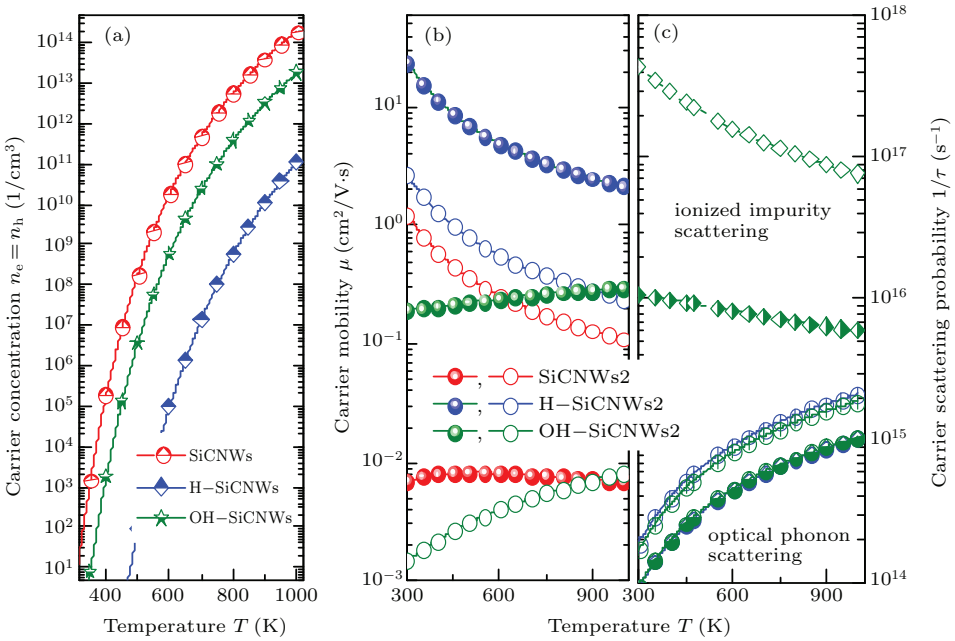


Fig. 4. Temperature-dependent (a) carrier concentration and (b) mobility of bare and passivated SiCNWs, with solid symbols representing electron mobility and hollow symbols denoting hole mobility; (c) temperature-dependent scattering probability of passivated SiCNWs.

3.3. Diameter-dependent conductivity

When the temperature is 300 K, the conductivity of bare SiCNWs decreases slowly with the increase of diameter, while the conductivity of the passivated SiCNWs increases rapidly as shown in Fig. 5(a). This opposite size dependence of the conductivity once again shows the inhibitory effect of dangling bonds on quantum size effect.[17]

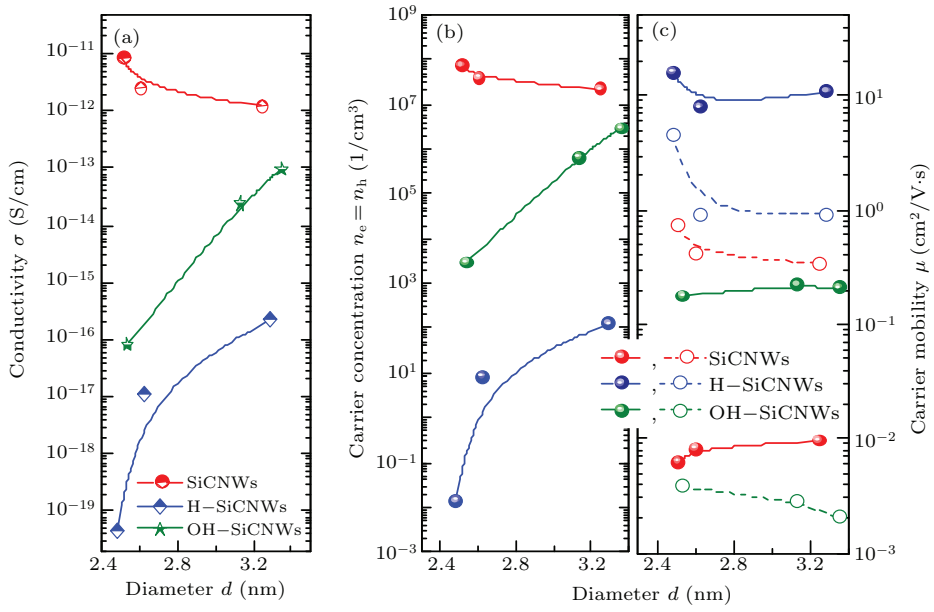


Fig. 5. (a) Diameter-dependent conductivity of bare and passivated SiCNWs, (b) diameter-dependent carrier concentration, and (c) diameter-dependent mobility of bare and passivated SiCNWs, with solid symbols representing electron mobility and hollow symbols denoting hole mobility.

The further analysis shows that the trend of conductivity varying with diameter originates from the size effect of band gap of SiCNWs, indicating that with the increase of diameter, the band gap of bare SiCNWs increases, which results in the decrease of intrinsic carrier concentration and the weakening of conductivity. For passivated SiCNWs, due to the fact that the band gap decreases with diameter increasing, both the intrinsic carrier concentration and the conductivity increase as shown in Fig. 5(b). It can be seen from Fig. 5(c) that the size effect of hole mobility at room temperature is more obvious than that of electron mobility. It can be found from Table 1 that the change of hole effective mass of SiCNWs with diameter is greater than the change of electron effective mass. Therefore, it can be believed that the strong size effect of the hole mobility at 300 K is due to the change of hole effective mass of SiCNWs with diameter. In addition, with the increase of diameter, the electron effective mass of H-SiCNWs increases (roughly) while that of OH-SiCNWs decreases, so the electron mobility of H-SiCNWs is different from that of OH-SiCNWs. Although the electron effective mass of SiCNWs is similar to that of H-SiCNWs, the electron mobility of SiCNWs is affected mainly by the density of electron states, so the trend of SiCNWs is different from that of H-SiCNWs.

4. Dielectric properties of different passivated SiCNWs

4.1. Orientation polarization relaxation of hydroxyl groups

Under the action of alternating electric field, the electron in semiconductor produces displacement polarization, and its dielectric constant can be written by Lorentz model as[8,24]

$$\varepsilon_r(\omega) = 1 + \frac{N_e e^2}{m_e^* \varepsilon_0} \frac{1}{\left(\omega_0^2 - \omega^2 - \mathrm{i}\gamma\omega\right)}, \tag{8}$$

where $\omega = E_g/\hbar$ is the circular frequency of the intrinsic transition (electron oscillation) and γ is the damping coefficient of electron oscillation. In a semiconductor with inherent dipoles, dipole orientation polarization produces relaxation. According to the Langevin's model and Debye's relaxation theory, the dielectric constant of hydroxyl passivated SiCNWs can be expressed as

$$\begin{aligned}\varepsilon_r(\omega) = {} & 1 + \frac{N_e e^2}{m_e^* \varepsilon_0} \frac{1}{\left(\omega_0^2 - \omega^2 - \mathrm{i}\gamma\omega\right)} \\ & + \frac{n_p p_0^2}{3\varepsilon_0 k_B T\left(1 - \mathrm{i}\omega\tau\right)} + \mathrm{i}\frac{\sigma}{\varepsilon_0\omega},\end{aligned} \tag{9}$$

where the dipole relaxation time is given below.

$$\tau = \frac{\pi}{2\nu_{ph}} \exp\left(-\frac{E_a}{k_B T}\right), \tag{10}$$

with E_a being the activation energy of polarization relaxation, which is related to the damping of orientation polarization.

4.2. Simulation of dielectric properties of different passivated SiCNWs

The dielectric properties of bare, hydrogen and hydroxyl passivated SiCNWs are numerically simulated according to Eqs. (8)–(10). The results are shown in Figs. 6 and 7.

Figure 6 shows that when the temperature is 300 K, hydroxyl passivated SiCNWs produce a relaxation response at 5.36 GHz, while the bare and hydrogen passivated SiCNWs do not. Figures 6(c) and 6(d) display the first-principles calculations, showing that the bare SiCNWs have a strong spectral response in blue light region, while the passivated SiCNWs present a more obvious spectral response in far-ultraviolet region.

Figure 7 shows the temperature characteristics and size effects of the dielectric constant of bare and passivated SiCNWs when the frequencies are 0.6 GHz, 5.36 GHz, and 10 GHz, respectively. It can be seen from Fig. 7(a) that the microwave dielectric constant of bare and hydrogen passivated SiCNWs are almost unchanged in the temperature range of 300 K–1000 K. When the temperature is higher than 400 K, the real part of the microwave dielectric constant of OH-SiCNWs2 decreases with temperature increasing, and when the temperature is higher than 550 K, the difference caused by frequency disappears. When the frequency is 0.6 GHz, the corresponding dielectric constant ε' increases with the temperature increasing in a range below 400 K, and the temperature at this inflection point shifts toward low temperature with the increase of frequency, which is shown in Fig. 7(a). Figure 7(b) exhibits that in the imaginary part of the dielectric constant corresponding to 0.6 GHz there appears a relaxation peak near 350 K, and the relaxation time decreases with the increase of frequency. As can be seen from Eq. (10), the corresponding temperature of the relaxation peak decreases, resulting in the relaxation peak of OH-SiCNWs2 appearing below room temperature.

As can be seen from Figs. 7(c) and 7(d), the microwave dielectric constant of hydroxyl passivated SiCNWs decreases linearly with the increase of diameter at room temperature ($T = 300$ K). As can be seen from Table 1, with the increase of SiCNW's diameter, the concentration of surface hydroxyl group decreases. According to Debye relaxation formula (9), the real part of the dielectric constant of OH-SiCNWs decreases with the increase of diameter. In addition, for the relaxation peaks corresponding to 5.36 GHz and 10 GHz at temperatures lower than room temperature, the imaginary part of the dielectric constant at 300 K also decreases with the increase of diameter as shown in Figs. 7(c) and 7(d).

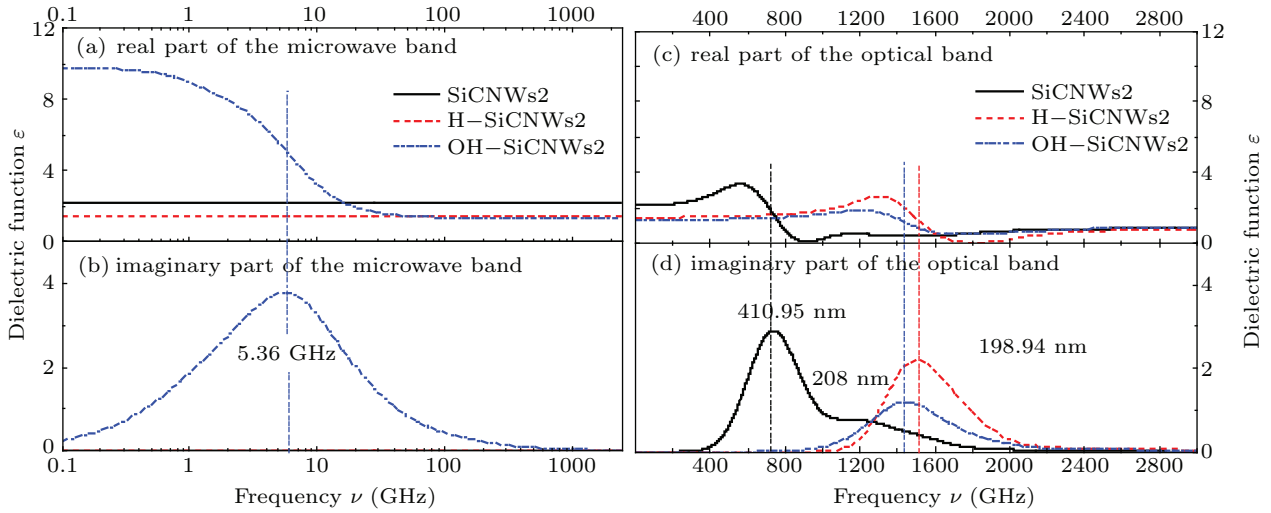


Fig. 6. Dielectric functions *versus* frequency for (a) real part and (b) imaginary part of microwave bands of bare SiCNWs2, and for (c) real part and (d) imaginary part of optical bands of passivated SiCNWs2.

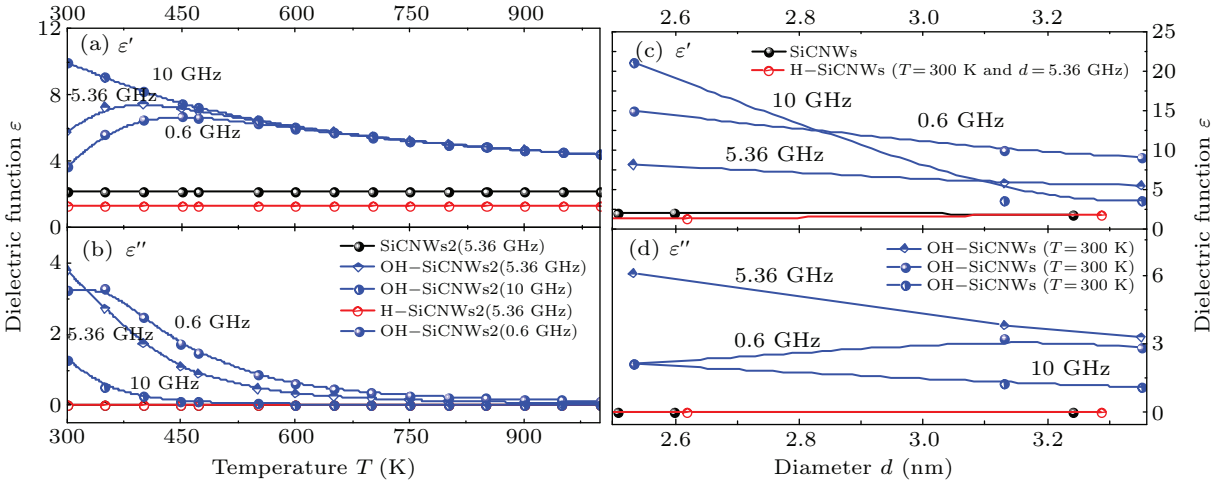


Fig. 7. Dielectric functions *versus* temperature for (a) real part and (b) imaginary part of dielectric constant of bare SiCNWs, and for (c) real part and (d) imaginary par of dielectric constant of passivated SiCNWs.

5. Conclusions

In conclusion, passivation results in the increase of the band gap of SiCNWs, in which hydrogen passivation increases the band gap of SiCNWs to a greater extent. Contrary to the size effect of bare SiCNWs, the band gap of passivated SiCNWs decreases with diameter increasing. The conductivity of SiCNWs, hydroxyl passivated SiCNWs and hydrogen passivated SiCNWs decrease in turn in the temperature range of 300 K–1000 K. Carrier concentration is a main factor affecting the conductivity of SiCNWs. The temperature dependence of hydrogen passivated structure is shown to be opposite to that of hydroxyl passivated structure. This is because optical phonon scattering plays a leading role in H-SiCNWs, while ionized impurity scattering plays a leading role in OH-SiCNWs. The trend of conductivity changing with diameter originates from the size effect of the band gap of SiCNWs, and the size effect of hole mobility at room temperature is more obvious than that of electron mobility. The bare SiCNWs have a strong dielectric response in the blue light region, while the passivated SiCNWs show an obvious dielectric response in the far ultraviolet-light region. The microwave dielectric constant of hydroxyl passivated SiCNWs decreases linearly with the increase of diameter at room temperature. This research is very meaningful for the applications of SiC nanomaterials in microwave electronic devices, and provides a theoretical basis for broadening the application of SiC nanomaterials as well.

References

[1] Konstantinos T, Thibaut B, Ni Y, Samy M, Xanthippi Z, Yann C, Patrice C and Sebastian V 2013 *Phys. Rev. B* **87** 125410
[2] Cheng G, Chang T H, Qin Q, Huang H and Zhu Y 2014 *Nano Lett.* **14** 754
[3] Casady J B and Johnson R W 1996 *Solid State Electron* **39** 1409
[4] Edmond J A 1988 *J. Electrochem. Soc.* **135** 2393
[5] Raynaud C 2001 *J. Non-Cryst. Solids* **280** 1
[6] Fan X, Ye R, Peng Z, Wang J, Fan A and Guo X 2016 *Nanotechnology* **27** 255604
[7] Kityk I V, Makowska-Janusik M, Kassiba A and Plucinski K J 2000 *Opt. Mater.* **13** 449
[8] Yang Y Y, Gong P, Ma W D, Hao R and Fang X Y 2021 *Chin. Phys. B* **30** 067803

[9] Xin X, Yan F, Koeth T W, Joseph C, Hu J, Wu J and Zhao J H 2005 *Electron. Lett.* **41** 1192
[10] Trew R J, Yan J B and Mock P M 1991 *Proc. IEEE* **79** 598
[11] Pham-Huu C, Keller N, Ehret G and Ledoux M J 2001 *J. Catal.* **200** 400
[12] Gong P, Yang Y Y, Ma W D, Fang X Y, Jing X L, Jia Y H and Cao M S 2021 *Physica E* **128** 114578
[13] Ma W D, Liu W K, Gong P, Jia Y H, , Yang Y Y and Fang X Y 2021 *Int. J. Mod. Phys. B* **35** 2150207
[14] Gendron F and Porter L M 1995 *Appl. Phys. Lett.* **67** 1253
[15] Trejo A, Calvino M and Cruz-Irisson M 2010 *Int. J. Quantum Chem.* **110** 2455
[16] Cuevas J L, Trejo A, Calvino M, Carvajal E and Cruz-Irisson M 2012 *Appl. Surf. Sci.* **258** 8360
[17] Li Y J, Li S L, Gong P, Li Y L, Fang X Y, Jia Y H and Cao M S 2018 *Physica B* **539** 72
[18] Cuevas J L, De Santiago F, Ramírez J, Trejo A, Mirandaá, Pérez L A and Cruz-Irisson M 2018 *Comp. Mater. Sci.* **142** 268
[19] Javan M B 2015 *Physica B* **456** 321
[20] Jia Y H, Gong P, Li S L, Ma W D, Fang X Y, Yang Y Y and Cao M S 2020 *Phys. Lett. A* **384** 126106
[21] Li Y L, Gong P and Fang X Y 2020 *Chin. Phys. B* **29** 037304
[22] Li S L, Yu X X, Li Y L, Gong P, Jia Y H, Fang X Y and Cao M S 2019 *Eur. Phys. J. B* **92** 155
[23] Li Y J, Li S L, Gong P, Li Y L, Fang X Y, Jia Y H and Cao M S 2018 *Physica E* **104** 247
[24] Gong P, Yang Y Y, Ma W D, Fang X Y, Jing X L and Cao M S 2021 *Opt. Mater.* **117** 111148